ASI

Carbon – Science and Technology

ISSN 0974 – 0546

http://www.applied-science-innovations.com

RESEARCH ARTICLE Received:13/09/2015, Accepted:02/10/2015

Characterization of phosphoric acid modified activated carbon fiber from fiber waste of pineapple leaf fiber production processing

Sumrit Mopoung [*], Pornsawan Amornsakchai, Sarocha Somroop

Department of Chemistry, Faculty of Science, Naresuan University, Phitsanulok, Thailand.

Abstract: Production of activated carbon fibers from fiber waste of pineapple leaf fiber production with phosphoric acid modification by non pre-carbonization activation and pre-carbonization activation processing were studied. The influences of step procedures, carbonization temperature (500 - 700 °C) and activation temperature (500 - 700 °C) on the resulting activated carbon fibers properties were evaluated. The non pre-carbonization activation is activation of fiber waste with H_2PO_4 of 1:1 ratio at 500-700 °C. For the pre-carbonization activation, it consisted of the carbonization of fiber waste at 500 °C followed by an activation step with H_2PO_4 of 1:1 ratio at 500 °C - 700 °C. The carbonized and activated products were characterized by SEM- EDS, FTIR, XRD and BET. It was found that percent yields of carbonization and activation products are decreased with increasing carbonization and activation temperature from 500 ^oC to 700 ^oC. Percent yield of the non pre-carbonization activated carbon and pre-carbonization activated carbon, which have high content of phosphorus 17.56 - 22.60 wt.%, are much higher than carbon from fiber waste (1.52 - 1.66 wt.%). The both activated carbons are oxygen- and phosphorus-containing groups on the sureface. After carbonization, the all samples are in form groove and streak ridge in parallel follow longitudinal of fibers with uneven and rough, and more broken and contracted after activation. The P, Si, K and Ca elements existed in activated carbon fiber. The best temperature in activation of fiber waste by both activation processes were 600 ^oC.

Keywords: Activated carbon fiber, fiber waste, pineapple leaf fiber production, phosphoric acid

1 Introduction: Plant fibers, which have been used by man for many generations, have remained an attractive material for a variety of potential applications. These fibers possess a distinctive characteristic, which makes them excellent materials for soil conservation, textile applications, as alternate materials especially wood substitutes in the construction market and as reinforcement of composite materials to produce automotive structural components [1]. Sources of plant fibers include jute and coconut fibers [2], empty fruit bunch fiber [3] and pineapple leaf [4]. Pineapple is largely cultivated in tropical countries, such as China, India, Thailand, Indonesia, and Taiwan. Normally leaves on farmland are used as a natural compost material or burned on site after the harvest, creating a point source of air pollution. The major constituents of pineapple leaf are cellulose (70 % – 80 %), lignin (5–12 %), and hemicellulose [5]. It has high potential for many purposes. The pineapple leaf powder has been used for adsorption of methylene blue from aqueous solution by Weng et al. [5]. It is also a source of high quality natural fiber and has many potential applications similar to other natural fibers such as plastic reinforcement, sound and thermal insulations [4], because the leaves of the pineapple plant yield strong, fine silky fibers. Such uses of pineapple leaves are doubly beneficial, providing a natural adsorbent and decreasing the amount of agricultural waste [5]. Utilization of pineapple leaf fiber waste for activated carbon fiber production not only converts the waste into a useful material but it also

prevents on-site burning of the waste and saves on disposal costs. Conventional methods for pineapple leaf fiber extraction such as scraping, retting and decorticating with a decorticator start from long fresh leaf and use mechanical force to remove soft covering material to provide long fibers [4]. Activated carbon fibers with high surface area and micropores have been prepared from hemp (*Cannabis sativa* L.) bast [6], jute and coconut fibers [2] empty fruit bunch fiber [3] and cellulose [7].

The textural characteristics of activated carbon fiber are not the only parameters affecting the adsorption. The chemical surface groups are also affected to adsorption activity [8]. Surface chemistry of activated carbon had been modified by oxidation with different oxidizing agents, which created functional groups such as quinine, diketone, chromene, pyrones, hydroxyl, carbonyl, carboxyl and phenolic groups [9]. The phosphoric acid is one activating agent for stable oxygen-containing groups and phosphorus-containing groups creating in the activated carbon, which retained and incorporated into activated carbon although intensive acid washing [10].

The aim of this research was to evaluate the potential of fiber waste from pineapple leaf fiber production as a low-cost adsorbent. The activated carbon fiber with high content of phosphorus containing groups was produced by fiber waste from mechanical milling process of pineapple leaf fiber production, as carbon fiber precursor. The modification of H_3PO_4 via non pre-carbonization activation and pre-carbonization activation process, carbonization temperatures and activation temperatures were evaluated.

2. Materials and methods

2.1 Sample preparation

2.1.1 Fiber waste preparation: Fiber waste (FW) was collected from mechanical milling process for the pineapple leaf fiber production. For mechanical milling process, fresh pineapple leaves which containing approximately 80 % water were chopped into pieces of 5 - 8 mm long. These were then wet-milled with a ball-mill or a disc mill. Milled material was cleaned with tap water to obtain pineapple leaf fiber and FW [4]. FW was oven (SL 1375 SHEL LAB 1350 FX) dried at 105 °C for 6 hours and then kept in the plastic bag.

2.1.2 Activated carbon preparation

Non pre-carbonization activation: Accurately weight by analytical balance (Satorious Basci) of FWs were impregnated with 85 % phosphoric acid (AR grade, Lab scan) in 1:1 weight/volume impregnation ratio. The impregnated mixtures were oven dried at 105 °C for 1 day. The dried impregnated mixtures were then placed in a closed crucible (size 105/73, 102/70) and activated at 400, 500, 600 and 700 °C in electric furnace (Fisher Scientific Isotemp® Muffle Furnace). The temperature was increased with a rate of 10 °C/min up to the desired temperature and kept constant for 1 h. At last, the activated products were cooled to room temperature. The final products were kept in the desiccator with label FWNPAC.

Pre-carbonization activation: Pre-carbonization activation or two-step processing is includs of first carbonization step and second activation step.

Carbonization step: The dried FWs were carbonized at 500 °C - 700 °C with increased of a rate of 10 °C/min up to the desired temperature and kept constant for 1 h. The obtained of catbon form FW (FWC) were used for acivation in secound step. All FWCs were washed with 0.2 M HCl (AR grade, Lab scan) and then oven dried at 105 °C for 3 h.

Activation step: The activation step was also done by impregnating FWC with 85 % phosphoric acid in 1:1 weight/volume impregnation ratio. The impregnated mixtures were oven dried at 105 °C for 1 day.

The dried impregnated mixtures were also activated as well as the non pre-carbonization activation process. The final products were also kept in the desiccator with label FWPAC.

2.2 Analysis and characterization

2.2.1 Yield percentages and instruments analyses: The carbonized and activated products of both non pre-carbonization activation and pre-carbonization activation process were analyzed for yield percentages and characterized by a Fourier transform infrared spectrometer (Spectrum GX, Perkin Elmer), X-ray diffractometer (PW 3040/60, X' Pert Pro MPD), scanning electron microscope - energy dispersive X-ray spectrometer (PHILIPS LEO 1455 VP) and Brunauer Emmett Teller surface area analyzer (Micromeritics TriStar II). The ash content of all samples was also analyzed by methods of ASTM D 2866–94 [11].

2.2.2 FTIR analysis: The chemical characterization of functional groups on surface of the all samples was studied by a Fourier transform infrared spectrometer in the range 4000 cm^{-1} - 400 cm^{-1}, using pellets with samples dispersed in KBr [6].

2.2.3 SEM-EDS analysis: Scanning electron microscopy was used to visualize the surface morphology of the carbonized and activated products. The samples were coated with gold by a gold sputtering device for a clear vision of the surface morphology. Elements composition of the samples was also observed using scanning electron microscopy equipped with energy dispersive spectrometer. EDS spectrum showing elemental composition by scanning through surface of samples. The surface distributions were collected from SEM pictures using different magnifications.

2.2.4 XRD analysis: X-ray patterns of FW, the carbonized and activated products were recorded by X-ray powder diffractometer with a Cu tube anode.

2.2.5 BET measurement: Textural characteristics were determined by N_2 adsorption at -196 °C on Brunauer Emmett Teller surface area analyzer. The samples were degassed at 250 °C for 12 h under vacuum before the measurements. The specific surface areas were estimated by the multipoint Brunauere Emmette Teller (BET) equation.

3. Results and discussion

3.1 Percent yield: After carbonization and both activation processes, percent yields of carbonization and activation products are decreased with increasing carbonization and activation temperature from 500 ^oC to 700 ^oC (Table 1). For carbonization products, it was caused by volatile matter was more degraded as higher carbonization temperature. This can be also attributed to a greater gasifying action between oxygen and carbon that causes a higher degree carbon burn-off even at a lower combustion temperature [3]. However, it was showed that the FW is potential for char production. For activated products, the yield progressively decreased with increased activation temperature due to thermal degradation of the phosphocarbonaceous species and formation of volatile phosphorous-containing compounds [12]. It was observed that percent yield of FWPACs are lower than FWNPACs for all same activation temperature. This can be attributed to during non pre-carbonisation activation, addition of H_3PO_4 into raw FW facilitated the conversion of aliphatic compounds, such as cellulose and hemicellulose, to aromatic compounds which was harder to decompose and thus FWNPAC yield are lowering the burn-off. In pre-carbonization activation, most aliphatic compounds were decomposed during carbonization before they were converted into aromatic compound by acid treatment. Another possibility is the ash factor. After carbonization, more ash was produced on the char surface. After pre-carbonization activation, HCl in washing step dissolved and washed away the ash, then yield of products are more decreased [3]. Another observation is that the percent of FWNPACs are higher than FWC, in spite it is not carbonization. In this case, it was attributed to P-containing additives (H_3PO_4) which act as inhibitors for the oxidation of

carbon materials by decrease the number of sites where carbon oxidation can take place [13]. Another cause, phosphoric acid hydrolyzes glycosidic linkages in hemicellulose and cellulose, and produces rupture of ether linkages in the structure of lignin, which explained by Romero-Anaya et al. [10]. This results in fractionation of biopolymers, structural weakening and redistribution of precursor material by combining with organic species to form phosphates or polyphosphates joints that connect and intersect the fragments of biopolymers. In addition to the dehydrating effect of phosphoric acid for the rupture of these bonds, it can form phosphate or polyphosphate esters with chain degraded biopolymers. The products of these reactions do not escape as volatile matter at low temperatures, but are retained and incorporated into the final solid residue. Therefore, FW impregnation with phosphoric acid produced an increase in the activation carbon yield in activation.

Table (1): Percent yield (proximate analysis), ash content and elements composition of samples by EDS analysis.

Samples	% yield	% ash	Wt.% of elements					
			C	O	Si	P	K	Ca
FW	-	1.15	49.03	45.54	1.16	1.15	0.93	0.86
FWC at 500 °C	28.51	3.55	68.27	22.61	1.62	1.66	3.87	1.96
FWC at 600 °C	24.12	5.28	73.42	16.90	1.78	1.73	2.41	1.80
FWC at 700 °C	19.65	9.59	75.53	16.71	1.01	1.52	4.07	1.15
FWNPAC at 500 °C	82.41	14.62	41.70	34.02	1.45	22.60	0.53	1.03
FWNPAC at 600 °C	80.75	14.75	41.92	34.11	1.58	21.99	0.63	0.60
FWNPAC at 700 °C	75.38	17.36	44.25	35.14	1.42	17.74	0.86	0.59
FWPAC at 500 °C	78.57	14.71	42.22	34.97	1.30	18.86	1.57	1.08
FWPAC at 600 °C	72.44	17.01	44.08	32.57	1.15	17.56	1.00	1.72
FWPAC at 700 °C	66.82	18.31	46.63	31.36	1.15	17.76	0.94	0.97

3.2 Ash content and element analysis: After carbonization and activation process, the carbon content of FWC increased, but the oxygen content revealed the opposite trend compared to the FW (Table 1). In this result, it was due to thermal degradation corresponding to oxidative pyrolysis. It also means enhances the nature of carbonaceous char, which is ideal for better activated carbon quality due to the removal of volatile compounds after carbonization process. In H_3PO_4 activation condition, H_3PO_4 helped in facilitating the removal of volatile [3]. It was observed that the carbon contents of FWNPAC and FWPAC are lower than FWC. Because of during the activation step, the oxidation effect of H_3PO_4 involves an increase in O content and a decrease in C content [2]. The presence of oxygen leads to further decomposition of secondary organic matter at higher temperatures and changes morphology of the produced char, thus leaving a deep impact on the combustion characteristics [3]. In addition, it may be caused of increasing oxygen and phosphorus contents form H_3PO_4 addition [12], which incomplete oxidation undergo lower 700 °C [2]. Another cause, it was due to the progressive formation of phosphates/polyphosphates bound to the carbon via C-O-P linkages within the temperature range of 500 °C - 700 °C [12]. The Si, K and Ca contents from raw FW were also observed in the FWCs, FWNPACs and FWPACs. The compounds of these elements are chemically stable and could survive extensive washing after carbonization or activation processes [12].

For ash content of all samples, it was increased with increasing temperature of carbonization and activation. It was due to the removal of volatile compounds from materials after carbonization and activation processes [3]. It was seen that the ash contents of FWNPACs are quite lower than that expected as compare with FWPACs. In this result, it could explain that the ash content was analyzed at > 800 °C, which phosphorus compounds and phosphorus element of FWPAC are thermal instability [12].

3.3 Spectra FTIR

3.3.1 Spectrum FTIR of FW: The FTIR spectrum of FW (Figure 1a) showed a high-intensity transmission band between 3200 and 3600 cm^{-1} with a maximum at about 3400 cm^{-1}. It was attributed to the –OH vibrational frequencies of hydroxyls bound to lignin [12] and the hydrogen-bonded OH vibration of the cellulosic structure [5]. The strong and sharp peak at about 2920 cm^{-1} attributed to the C–H stretches of methyl and methylene groups of cellulose and hemicellulose [12]. The peak at 1737 cm^{-1} is due to C–O stretching of carbonyl groups (>C=O) in hemicellulose [5]. The peak at 1430 cm^{-1} could be ascribed to $–CH_2–$ scissoring vibration [14] and the in-plane symmetric deformation vibration of $–CH_3$ in lignin [5] and the band at 1373 cm^{-1} is related to the in-plane bending vibrations of O–H or stretching of C=O in cellulose [6], and the shoulder at 1232 cm^{-1} corresponds to the asymmetric stretching of =C–O–C connected with aryl groups in hemicellulose structures [5]. The sharp and weak peak at 1160 cm^{-1}, high-intensity peak at 1055 cm^{-1}, very weak peak at 897 cm^{-1} and weak band at 612 cm^{-1} attributed to the asymmetric stretching vibration of C–O bond in ester group, aromatic C–H in-plane deformations, in-plane bending vibrations of C–H or out-of-plane deformation mode of C–H and O–H in pyranoid rings involved in cellulose structure or polysaccharide molecules, and the out-of-plane deformation mode of O-H of cellulose [14], respectively. Finally, the small peaks between 600-500 cm^{-1} in the spectra of the FW refers to typical cellulose structures and correspond to aromatic ring C–H groups in the lignin [15].

3.3.2 Spectra FTIR of FWCs: The weak band at 3400 cm^{-1} observed for FWCs (Figure 3 b-c) illustrating decreased in the number of OH-groups present after carbonization at 500-700 ^oC [12]. The peak at 1738 cm^{-1} of only FWC with activation at 700 ^oC could be assigned to the stretching vibrations of C=O in ketones, carboxylic acids or isolated carbonyl groups that are not involved in conjugation with a double bond or aryl group [6]. This is because that –OH groups are removed in gaseous form by pyrolytic decomposition of FW during thermal treatment, which are oxidized to C=O groups and COO– groups [14]. It was revealed that these functional groups created after carbonization at 600 ^oC. The band at 1561-1582 cm^{-1} ascribed to the aromatic ring stretching vibrations (C=C) [14]. This band was appeared by loss of oxygen-functionalities and aromatic condensation [16]. The band at 1361-1376 cm^{-1} and 1216-1217 cm^{-1} are attributed to C–H deformation in the typical carbohydrate of cellulose and hemicellulose and the guaiacyl-type lignin [16], which still remained in FWCs. However, they disappeared gradually from 500 ^oC to 700 ^oC. Three quite weak shoulder peaks at 874, 810 and 757 cm^{-1}, respectively, all of which are related to the out-of-plane bending vibrations of C-H in aromatic rings with a large degree of substitution. This aromatic C–H band becomes so weak that it is even not readily observable with increasing the carbonization temperature, demonstrating a progressive substitution of C–H bonds in the aromatic system and the formation of new C–R bonds [6] or probably by an increase in the degree of aromatic condensation [17]. All these peaks, except peak at 1738 cm^{-1}, are gradually decreased intensity with increase carbonization temperature from 500 ^oC to 700 ^oC.

3.3.3 Spectra FTIR of FWNPACs and FWPACs: The FTIR spectrum of all of FWNPACs (Figure 3 e-g) and FWPACs (Figure 3 h-j) showed much less intense transmission bands than all of FWCs and FW. These clearly show the activating function of phosphoric acid that facilitates a restructuring of the organic precursor to a carbon structure. After H_3PO_4 activation between 500 ^oC and 700 ^oC, both of all FWNPACs and FWPACs showed broader band and also weak signal in the 3200–3600 cm^{-1} region, which is characteristic of the stretching vibration of hydrogen-bonded hydroxyl groups of carboxyls, phenols or alcohols and also OH-groups [12]. The peak at about 2920 cm^{-1}, 1216-1582 cm^{-1}, and 757-874 cm^{-1} disappeared after activation. It was indicated that phosphoric acid promotes further removal of any remained functional groups from FWC structure. The small and weak band at 2348-2374 cm^{-1} of all FWNPACs and FWPACs, which quite higher intensity than FWCs corresponds to P-H vibrations [18].

The very weak band at 1737–1739 cm^{-1} of FWNPAC and FWPAC with activation at 700 °C were assigned to C=O stretching in non-conjugated and conjugated systems (carbonyl/carboxyl groups) [16]. It revealed that have more oxidation with H_3PO_4 at 700 °C. All the spectra of activated carbon fibers also showed an band at about 1584-1638 cm^{-1} due to the C=O stretching in quinones [6] and aromatic rings [12], which gradually decreased as activation temperature increase from 500 °C to 700 °C. The band at 1144–1154 cm^{-1} can be assigned to the stretching vibration of hydrogen bonded P=O groups of phosphates or polyphosphates, O–C stretching vibration in the P–O–C (aromatic) linkage, P=OOH and the symmetric stretching mode of O–P–O non-bridging oxygens which indicate the formation of phosphate tetrahedral [19]. The peak at 1003–995 cm^{-1} may be due to aliphatic P–O–C stretching, aromatic P–O–C asymmetric stretching, P–O stretching in >P=OOH, P–OH bending, P–O–P asymmetric stretching in polyphosphates, and symmetrical stretching of P–O present in phosphate–carbon complexes [12]. It also due to the symmetric stretching mode of non-bridging oxygens in phosphate tetrahedral [19]. The very weak peak at 887 cm^{-1} which appeared after activation with H_3PO_4, is related to silanol groups (Si–O containing groups) [20] which came from raw FW and also to asymmetric stretching of P–O–P groups. It attributed that the phosphate group is built from short chains containing phosphorus-oxygen and pyrophosphate groups $P_2O_7^{4-}$ [19]. The last band at about 490 cm^{-1} found in all of the FWNPACs and FWPACs corresponds to P^+–O^- vibrations [21], which appeared after activation with H_3PO_4. It indicated that the change in pyrophosphate group to orthophosphate group [19]. Thus, the FT-IR analysis confirms the existence of oxygen- containing groups and phosphorus-containing groups in the activated carbon fibers and corresponds to EDS data (Table 1).

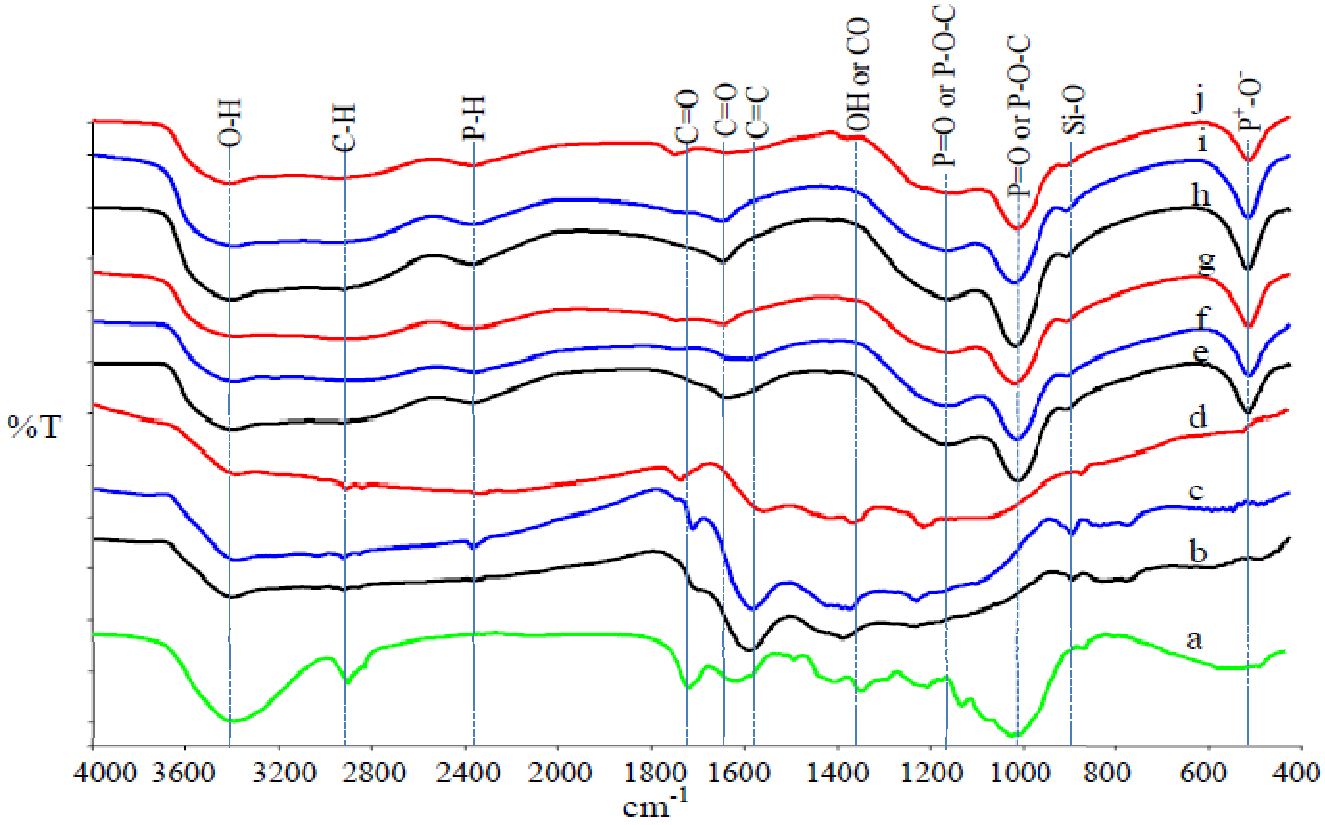

Figure (1) FTIR spectra of (a) FW (b) FWC at 500 °C (c) FWC at 600 °C (d) FWC at 700 °C (e) FWNPAC at 500 °C (f) FWNPAC at 600 °C (g) FWNPAC at 700 °C (h) FWPAC at 500 °C (i) FWPAC at 600 °C (j) FWPAC at 700 °C.

3.4 SEM Morphology: SEM micrographs of FW and FWCs are illustrated in Figure 2 a-d. The FW (Figure 2 a), which used as raw material showed in form of bundles with highly packed, some pits and holes on the surface. After carbonization at 500-700 ^{o}C, the FWCs are in form groove and streak ridge in parallel follow longitudinal of fibers with uneven and rough (Figure 2 b-d) as compared with FW. These FWCs (diameter 4-25.33 µm) were thinner than FW (diameter ~34.67 µm). It attributed to thermal degradation of volatile matter [22]. As higher carbonization temperature, there are the broken and flat of FWCs (Figure 2 c-d). They were form through the decomposition of volatile matters followed by densification during carbonization process [3]. There were also a number of opening pore channels in the samples (Figure 3b), which similar to hemp fiber [23] and oil palm empty fruit bunch fiber [3]. The FWNPACs and FWPACs are seems to more broken and contracted than the FWCs of the same temperature. It may be attributed to contraction by higher dehydrating of phosphoric acid during activation process and the cause of the destruction of the morphology in both FWNPACs and FWPACs [10].

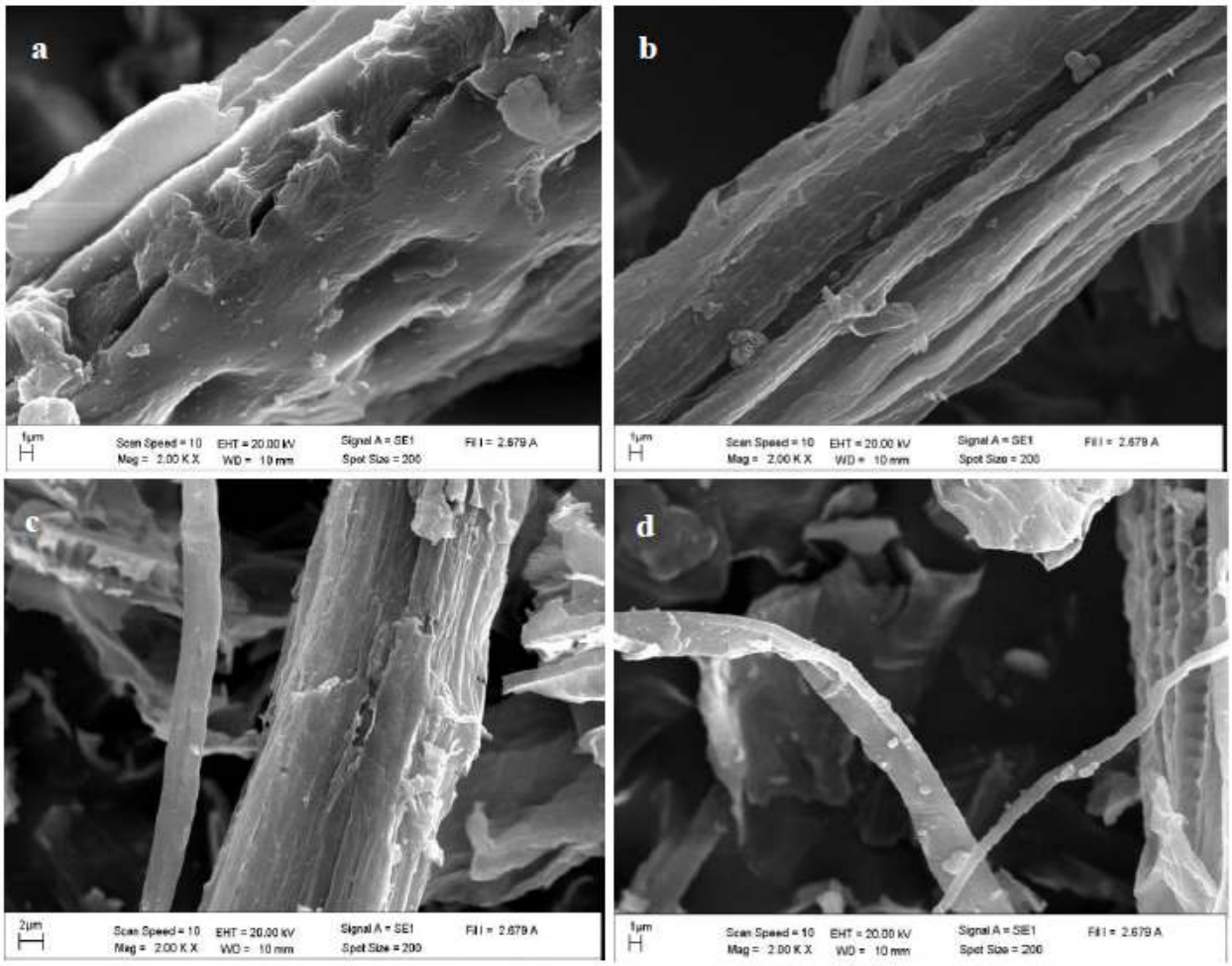

Figure (2): SEM micrographs of (a) FW (b) FWC at 500 ^{o}C (c) FWC at 600 ^{o}C (d) FWC at 700 ^{o}C.

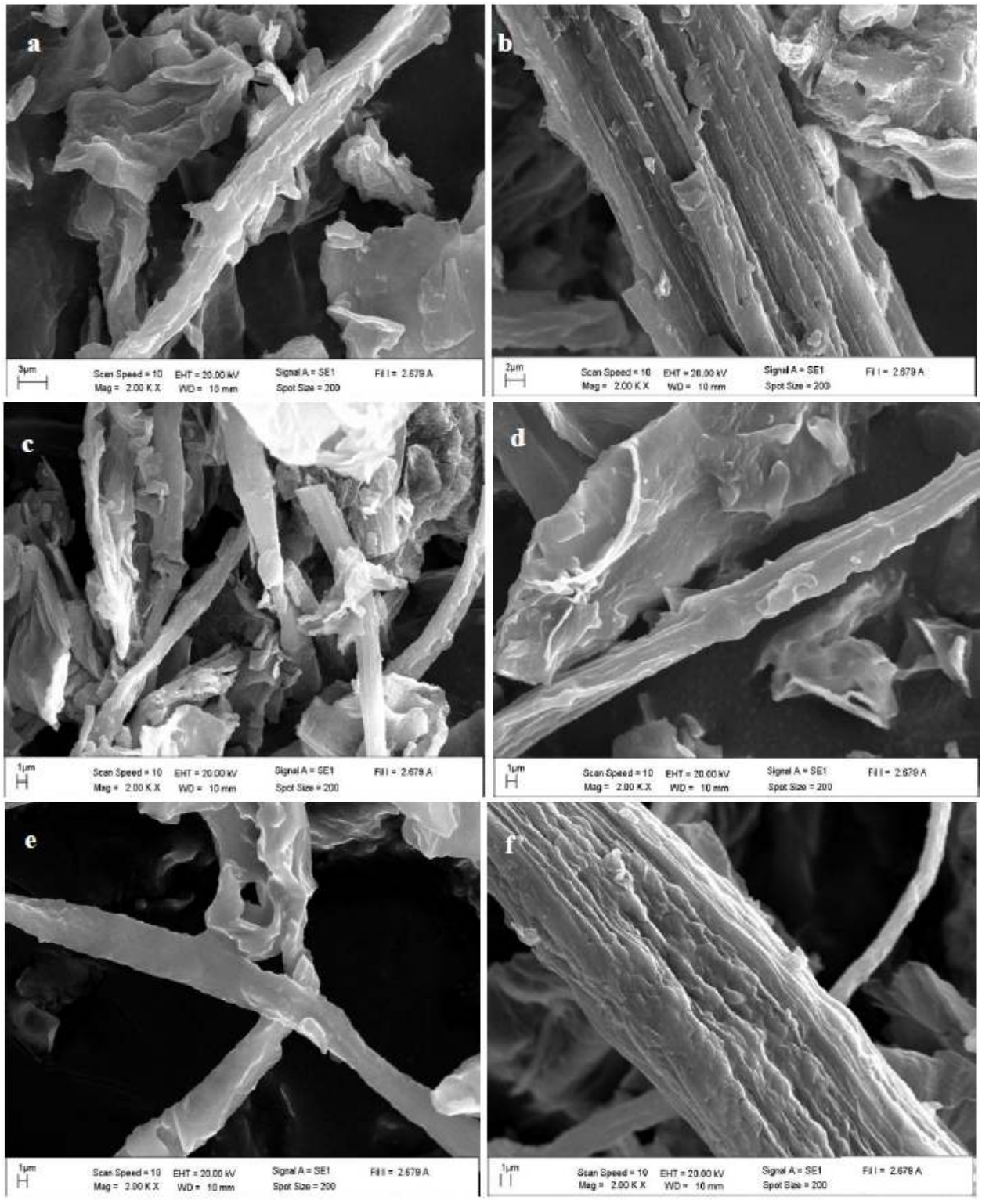

Figure (3): SEM micrographs of (a) FWNPAC at 500 ^{o}C (b) FWNPAC at 600 ^{o}C (c) FWNPAC at 700 ^{o}C (d) FWPAC at 500 ^{o}C (e) FWPAC at 600 ^{o}C (f) FWPAC at 700 ^{o}C.

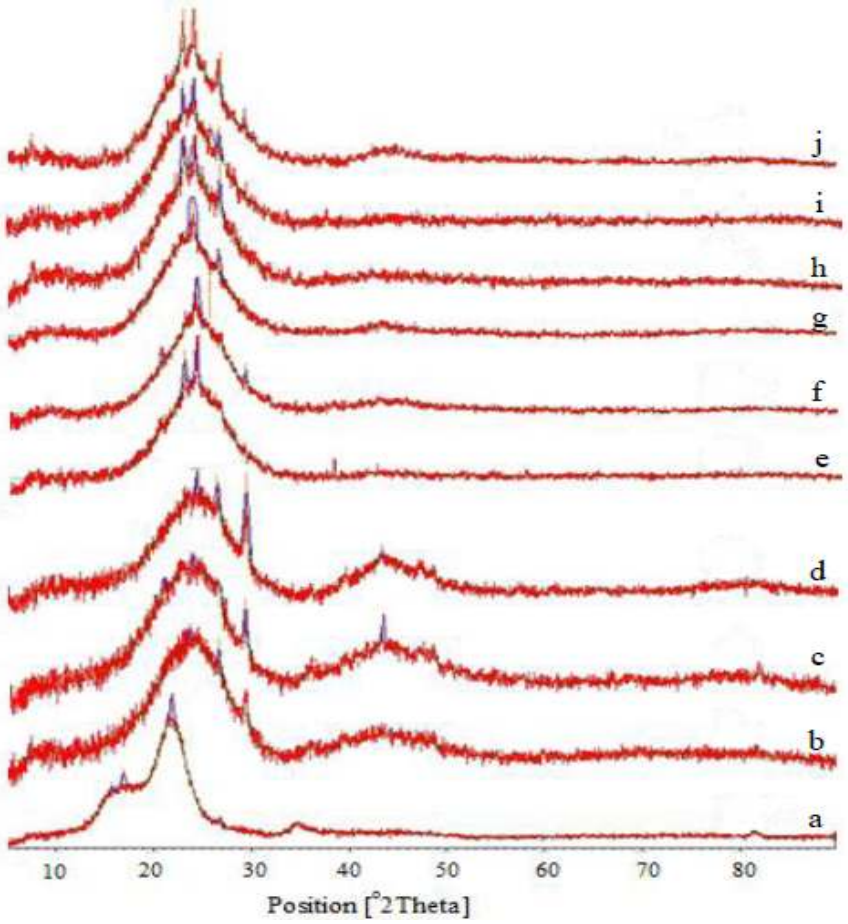

Figure (4): X-ray diffractograms of (a) FW (b) FWC at 500 °C (c) FWC at 600 °C (d) FWC at 700 °C (e) FWNPAC at 500 °C (f) FWNPAC at 600 °C (g) FWNPAC at 700 °C (h) FWPAC at 500 °C (i) FWPAC at 600 °C (j) FWPAC at 700 °C.

Table (2): BET surface area, pore volume, pore size and micro pore area of samples.

Samples	BET surface area (m^2/g)	pore volume (cm^3/g)	Average pore size (nm)
FWC at 500 °C	48.4335	0.03076	2.5402
FWC at 600 °C	183.8400	0.10075	2.1921
FWC at 700 °C	413.3908	0.21747	2.1043
FWNPAC at 500 °C	11.0337	0.03655	13.2514
FWNPAC at 600 °C	16.6105	0.07991	19.2423
FWNPAC at 700 °C	5.4918	0.02576	18.7608
FWPAC at 500 °C	0.8274	0.00122	5.8809
FWPAC at 600 °C	0.6090	0.00071	4.6382
FWPAC at 700 °C	1.9465	0.00372	7.6416

3.5 XRD analysis: FW clearly presents diffraction peaks around 2θ = 15.5, 16.5, 22.5 and 34.5° (Figure 4a), corresponding to cellulose of I type allomorph [24]. Cellulose is identified by the characteristic peaks of crystalline fraction at 2θ degrees between 22° and 23° and that correlated to the amorphous fraction at 2θ degrees between 15° and 16° [25]. It also shows very weak diffraction peaks of a little amount of starch at 15.2° and 17.2° [26]. The broad diffraction peak of FW with a maximum at about 2θ = 22° with overlap to peak of cellulose is also typical lignin [27]. It is observed that the intensity of diffraction peaks of FW decreases with increasing temperature, shifting the diffraction peaks toward a

greater spacing. It can be explained due to the progressive deterioration of cellulose crystal lattice, until the structure becomes completely amorphous [24], observed for FWCs (Figure 4 b-d).

All FWCs (Figure 4 b-d), FWNPACs (Figure 4 e-g) and FWPACs (Figure 4 h-j) had two broad peaks at 24° and 43° which were assigned to the disordered carbon structure [28]. Peak quite dominant at 27° were assigned to silicate in form of α-quartz (Si_3O_6) [29]. The sharp peak at 29.5° and small peak at 34.5° attributed to calcium compound [30] and potassium compound [31], respectively. Finally, the sharp peak at about 25° of FWNPACs and FWPACs is a diffraction peak of P-C [32], which is attributable to distortion in the crystalline regularity and to vacancies caused by the introduction of P atoms [33] into FWNPACs and FWPACs. These results are confirmed that the P, Si, K and Ca elements are in FWCs, FWNPACs and FWPACs. Including, the reactivity of H_3PO_4 to FW or FWC is effect to structural, textural and chemical with increases in the degree of structural disorder.

3.6 BET measurement: BET surface area and pore volume of FWCs were trend increased with increasing carbonization temperature from 500 ^oC to 700 ^oC. In the other hand, pore size was trend reversed. It is because of dehydration and degradation occurs and subsequently, oligomeric products of its transformation with the resulting formation of carbon framework with large porosity and causing the formation of ordered mesoporous carbon structures [22]. After activation, all both FWNPACs and FWPACs are much lower surface area and pore volume than FWCs. In this result, it attributed to H_3PO_4 promoted bond cleavage reactions and formation of crosslink by combining with the lignocellulosic polymers, which phosphate linkages, such as phosphate and polyphosphate esters connect and bind strongly to the biopolymer matrix [34]. Therefore, the phosphorus compounds were increased the retention within the structure and covered the surface of activated carbon. Another reason attributed to contraction occurs by catalytic activity of phosphoric acid, which allows the growth and alignment of polyaromatic clusters, producing a more densely packed structure and some loss of porosity [12]. However, pore sizes of them, except FWNPAC at 700 ^oC, are more expanded and trend increase the width as increase activation temperature from 500 ^oC to 700 ^oC. The decrease in surface area and pore volume of FWNPAC at 700 ^oC were due to the breakdown, restructuring and constriction of the pore walls and pore apertures [34]. The pore sizes of FWPACs are much narrower than FWNPACs, but much wider than FWCs. However, the average pore sizes of all samples are in a range of mesopore [34]. It could be explained that volatile phosphorus-based compounds (phosphorus(V) oxide and elemental phosphorus), which form at high temperature were volatiled and served pore size increasing [12]. For effects of activation processes, because of phosphoric acid dissolved and washed away the ash, then intercalated onto the carbon surface, creating more wider pores by exfoliation during non pre-carbonization activation [3]. However, as the temperature increases to 700 ^oC, the contribution of the intercalation reaction progressively decreases leading to the decay of wider pores [35] of FWNPACs. It was observed that the average pore sizes of FWNPACs and FWPACs are also in a range of mesopore. These results agree with the report of Tehrani et al. [34], which used impregnation ratios of H_3PO_4 between 30 and 180 wt.% to the weight of materials and at < 800 ^oC, showed high amount of mesoporous volume. Highly interesting, the BET surface area of FWNPACs and FWPACs are very low as compared of FWCs. It confirmed that the surface of FWNPACs and FWPACs were cover with high amount of phosphorus compounds.

4 Conclusions: This research revealed that the FW can be used as a natural-based adsorbent with H_3PO_4 modification. It has been well established that the H_3PO_4 modification of FW is improve the oxygen-containing groups and phosphorus-containing groups on the surface of activated carbon fiber, such as: carbonyl, carboxyl, phenol, quinone, silanol, especially phosphates and polyphosphates groups. These functional groups are importance to the adsorption activity of activated carbon fiber. It expected that both of activated carbon fibers with H_3PO_4 modification are high adsorption capacity for removal the

heavy metal from aqueous solutions. It was concluded that the best temperature in activation of FW by both activation processes were 600°C.

Acknowledgement: This work was financially supported by Naresuan University. The authors acknowledge Science lap center, Faculty of Science, Naresuan University for all of the analysis.

References:

[1] S. Kalia, K. Thakur, A. Celli, M. A. Kiechel, C. L. Schauer, J. Environ. Chem. Eng. 1 (2013) 97.
[2] N. H. Phan, S. Rio, C. Faur, L. L. Coq, P. L. Cloirec, T. H. Nguyen, Carbon 44 (2006) 2569.
[3] T. Lee, Z. A. Zubir, F. M. Jamil, A. Matsumoto, F.-Y. Yeoh, J. Anal. Appl. Pyrol. 110 (2014) 408.
[4] N. Kengkhetkit, T. Amornsakchai, Ind. Crop. Prod. 40 (2012) 55.
[5] C.-H. Weng, Y.-T. Lin, T.-W. Tzeng, J. Hazard. Mater. 170 (2009) 417.
[6] R. Yang, G. Liu, X. Xu, M. Li, J. Zhang, X. Hao, Biomass Bioenerg. 35 (2011) 437.
[7] M. E. Ramos, P. R. Bonelli, A. L. Cukierman, Colloid. Surface. A 324(1–3) (2008) 86.
[8] M. Belhachemi, M. Jeguirim, L. Limousy, F. Addoun, Chem. Eng. J. 253 (2014) 121.
[9] D. Duranoğlu, A. W. Trochimczuk, Ü. Beker, Chem. Eng. J. 165 (2010) 56.
[10] A. J. Romero-Anaya, M. A. Lillo-Ródenas, C. Salinas-Martínez de Lecea, A. Linares-Solano, Carbon 50(9) (2012) 3158.
[11] American Standard of Testing Material. Standard Test Method for Total Ash content of Activate Carbon. ASTM D 2866-94 (1996).
[12] M. Myglovets, O. I. Poddubnaya, O. Sevastyanova, M. E. Lindström, B. Gawdzik, M. Sobiesiak, M. M. Tsyba, V. I. Sapsay, D. O. Klymchuk, A. M. Puziy, Carbon 80 (2014) 771.
[13] F. Suárez-García, A. Martínez-Alonso, J. M. D. Tascón, Fuel Process. Technol. 77–78 (2002) 237.
[14] J. Zheng, Q. Zhao, Z. Ye, Appl. Surf. Sci. 299 (2014) 86.
[15] H. Tibolla, F. M. Pelissari, F. C. Menegalli, LWT – Food Sci. Technol. 59(2) (2014) 1311.
[16] J. G. Pohlmann, E. Osório, A. C. F. Vilela, M. A. Diez, A. G. Borrego, Fuel 131 (2014) 17.
[17] A. M. Puziy, O. I. Poddubnaya, A. Martınez-Alonso, Carbon 41(6) (2003) 1181.
[18] F. H. Abdelghany, H. A. ElBatal, F. M. ElBatal, F. M. EzzElDin, J. Mol. Struct. 1074 (2014) 503.
[19] P. K. Jha, O. P. Pandey, K. Singh, J. Mol. Struct. 1083 (2015) 278.
[20] Y. Guo, D. A. Rockstraw, Micropor. Mesopor. Mat. 100(1–3) (2007) 12.
[21] N. V. Sych, S. I. Trofymenko, O. I. Poddubnaya, M. M. Tsyba, V. I. Sapsay, D. O. Klymchuk, A. M. Puziy, Appl. Surf. Sci. 261 (2012) 75.
[22] N. D. Shcherban, P. S. Yaremov, V. G. Ilyin, M. V. Ovcharova, J. Anal. Appl. Pyrol. 107 (2014) 155.
[23] J. M. Rosas, J. Bedia, J. Rodríguez-Mirasol, T. Cordero, Fuel 88(1) (2009) 19.
[24] M. Benítez-Guerrero, J. López-Beceiro, P. E. Sánchez-Jiménez, J. Pascual-Cosp, Thermochim. Acta 581 (2014) 70.
[25] L. Hajji, A. Boukir, J. Assouik, H. Lakhiari, A. Kerbal, P. Doumenq, G. Mille, M. L. De Carvalho, Spectrochim. Acta A 136 (2015) 1038.
[26] R.-L. Wu, X.-L. Wang, F. Li, H.-Z. Li, Y.-Z. Wang, Bioresource Technol. 100(9) (2009) 2569.
[27] V. Vivekanand, A. Chawade, M. Larsson, A. Larsson, O. Olsson, Ind. Crop. Prod. 59 (2014) 1.
[28] J. Jin, B.-J. Yu, Z.-Q. Shi, C.-Y. Wang, C.-B. Chong, J. Power Sources 272 (2014) 800.
[29] I. O. Ali, M. S. Thabet, K. S. El-Nasser, A. M. Hassan, T. M. Salama, Micropor. Mesopor. Mat. 160 (2012) 97.
[30] Y. Tianxue, Y. Li, H. Haobo, X. Beidou, H. Liansheng, W. Xiaowei, H. Caihong, W. Kun, Z. Ying, C. Bin, Bioresource Technol. 163 (2014) 356.

[31] J. Díaz-Terán, D. M. Nevskaia, J. L. G. Fierro, A. J. López-Peinado, A. Jerez, Micropor. Mesopor. Mat. 60/1–3 (2003) 173.
[32] J. Zhu, G. He, L. Liang, Q. Wan, P. K. Shen, Electrochim. Acta 158 (2015) 374.
[33] P. Song, X. Bo, A. Nsabimana, L. Guo, Int. J. Hydrogen Energ. 39/28 (2014) 15464.
[34] N. F. Tehrani, J. S. Aznar, Y. Kiros, J. Clean. Prod. 91 (2015) 64.
[35] P. Kleszyk, P. Ratajczak, P. Skowron, J. Jagiello, Q. Abbas, E. Frąckowiak, F. Béguin, Carbon 81 (2015) 148.

*****